G.J. Heij and J.W. Erisman (Editors). Acid Rain Research: Do we have enough answers?

The atmospheric input of inorganic nitrogen and sulphur by dry deposition of aerosol particles to a spruce stand

K. Peters[a] and G. Bruckner-Schatt[b]

[a]Bayreuth Institute for Terrestrial Ecosystem Research (BITÖK), Department of Climatology, University of Bayreuth, D-95440 Bayreuth, Germany

[b]Chair of Plant Ecology I, University of Bayreuth, D-95440 Bayreuth, Germany

Abstract

The dry deposition of particle-bound NH_4^+, NO_3^- and SO_4^{2-} to a spruce stand was determined by the inferential method. For determining the deposition velocity the model DEPOSITE was used, based on an analysis of the probability of absorption of particles on plant surfaces due to sedimentation, impaction and molecular diffusion through the laminar boundary layers.

The investigation stand was a 45 year old spruce forest with a mean tree height of 20 m and a *LAI* of 11.4. Airborne particle-bound concentrations of the main inorganic ions were measured as a function of the particle size by Berner cascade impactors mounted at the top of the canopy. From June to November 1992 a total of 23 samples were taken covering 23% of a whole year. In scaling up the input fluxes found for each sampling period to mean values for one year, the results were 2.6 kg NH_4^+-N ha^{-1} yr^{-1}, 2.8 kg NO_3^--N ha^{-1} yr^{-1} and 3.6 kg SO_4^{2-}-S ha^{-1} yr^{-1} which corresponds to 21% and 10% of the total atmospheric N and S input at this site.

1. INTRODUCTION

The input fluxes of particulate and gaseous nitrogen and sulphur compounds from the atmosphere to vegetation canopies are of major importance in considering the balance of nutrients and pollutants within ecosystems. The dry deposition of these elements is considered to be in the same order of magnitude as the wet deposition [1,2]. Of the dry deposition, the input of the trace gases NH_3, NO_x, HNO_3 and SO_2 is commonly larger than the flux of the particle-bound ions NH_4^+, NO_3^- and SO_4^{2-} [3]. Despite this fact the contribution of the particulate deposition cannot be neglected.

For determining the dry deposition of aerosol particles a large variety of methods have been proposed [4]. Among these, the sampling of deposited particles by surrogate surfaces [5–7] and the application of the throughfall method [8–10] are most commonly used. The latter suffers from the fact that the portion of ions in the throughfall water originating from leaching or from deposited trace gases is not well known. A shortcoming of surrogate surfaces arises from their aerodynamic properties, which are different from those of real plant leaves.

Some studies have dealt with the application of micrometeorological methods, the most important of which are the profile method and the eddy-correlation method [11–

14]. The use of these procedures within forested areas is often limited due to the insufficient fetch, especially at mountainous sites.

Recently, the *inferential method* has been established. It is an indirect method, but reduces the fetch requirements of the common micrometeorological methods. Here, a deposition velocity v_d is calculated from the micrometeorological conditions at the site and from parameters characterizing the plant morphology. According to the fundamental equation

$$F(d_p) = v_d(d_p, z)\, c(d_p, z) \tag{1}$$

the dry deposition flux F is the product of v_d and the airborne particulate concentration c which has to be measured above the canopy. The independent variables d_p and z are the particle aerodynamic diameter and a distinctive reference height above the canopy, respectively. If v_d is known from the model calculation, it is sufficient to measure c for determining the dry deposition.

This approach is widely used for trace gases, where v_d is usually expressed as the inverse of a resistance [15,16]. Studies dealing with v_d of aerosol particles normally do not calculate resistances, but are based on the combination of absorption probabilities [17–21]. In this study the model DEPOSITE, a further development of these approaches, was used [22]. It is mainly based on the work of Bache [17–19] who dealt with the deposition of water droplets. In extending the applicability of this model to the whole size range of natural aerosol particles a description of the particle diffusion through laminar sublayers surrounding all plant surfaces was added.

The model was used to calculate the dry deposition of the main particulate inorganic ions to a Norway spruce canopy at Wülfersreuth in the mountainous region Fichtelgebirge in northeastern Bavaria, Germany.

2. MATERIALS AND METHODS

2.1. The model DEPOSITE

The model DEPOSITE, which calculates the size specific deposition velocity of aerosol particles to coniferous forests, was explained in detail by Peters and Eiden [22]. Important featured will be repeated here.

Neglecting advection and assuming that the mean vertical wind velocity is zero, the mechanisms governing the transport of particles through the canopy are *turbulent diffusion*, *sedimentation* and *absorption at plant surfaces*. In combining these processes, the mass balance within an elemental volume of the canopy is considered. The result is a differential equation describing the vertical gradient of the airborne particle concentration [17]:

$$\frac{d^2c}{dz^2} + f(z)\frac{dc}{dz} + g(z)c = 0 \tag{2}$$

with

$$f(z) = -\frac{v_s}{K(z)} + \frac{1}{K(z)}\frac{dK(z)}{dz} - \beta(z)\rho(z)\sin\varphi(z) \tag{3}$$

and

$$g(z) = -\frac{\beta(z)\rho(z)}{K(z)}\sqrt{u(z)^2 + v_s^2}. \tag{4}$$

In these equations v_s is the sedimentation velocity, u is the horizontal wind velocity, and K is the turbulent diffusivity of aerosol particles. φ is the angle of the particle trajectory to the horizontal and can be expressed by $\varphi = \arctan(v_s/u)$. ρ is the vegetation density defined as total surface area of the plant elements per volume of the canopy. β is the absorption coefficient which combines the absorption efficiencies due to diffusion, impaction and sedimentation.

If both height specific functions $f(z)$ and $g(z)$ are replaced by representative constants f_R and g_R, Equation (2) can be solved analytically [18]. However, in order to make the solution more exact the canopy can be subdivided in several horizontal layers i with equal thickness Δz. Now for each of these height intervals individual constants f_{Ri} and g_{Ri} can be determined. This procedure, proposed by Bache [19], was used in this study.

The calculation of the deposition velocity can then be treated as an initial value problem starting at the lowest height interval. The solution proceedes through all layers to the top of the canopy, finally calculating the overall deposition velocity v_d.

The absorption coefficient β is determined by a probabalistic analysis considering diffusion, impaction and sedimentation as well as the mutual interferences between these processes. The result is

$$\beta = 1 - (1 - P_z)^{(1/(1+u^2/v_s^2))^{1/2}}[(1 - P_{x,\mathrm{di}})(1 - P_{x,\mathrm{im}})]^{(1/(1+v_s^2/u^2))^{1/2}}, \tag{5}$$

where $P_{x,\mathrm{di}}$, $P_{x,\mathrm{im}}$ and P_z are the absorption probability due to diffusion, impaction and sedimentation, respectively. While diffusion and impaction are controlled by the horizontal movement of the particles (denoted by the subscript x), sedimentation occurres during the movement in the z-direction. Other processes like interception, resuspension and bounce-off are less important for coniferous needle surfaces during moderate wind conditions and will be neglected.

In this paper *diffusion* denotes the processes responsible for the transport of particles through the laminar boundary layer that surrounds all surfaces. The diffusion term used in the model is expressed as a function of the friction velocity u_* in the vicinity of the plant surfaces. The approach is based on the equation from Friedlander and Johnstone [23] who described the diffusion flux with respect to the molecular diffusivity within the boundary layer and some turbulent portion also contributing to the transfer. Additionally, the microscale roughness of the plant surfaces was introduced since it reduces the thickness of the boundary layer [24]. Moreover, the effect of so-called *bursts* within boundary layers, first observed by Kline *et al.* [25], was considered. Downward sweeps of air compensating for these bursts transfer momentum to the particles, pushing them towards the surface.

For describing the *impaction* of particles upon obstacles like needles an empirical approach is used which expresses the absorption probability as a function of the Stokes number. The equation was found to fit well to the experimental results of May and Clifford [26] and Belot and Gauthier [27].

The *sedimentation* is characterized by the terminal velocity v_s of settling particles, when the gravitational force and the drag force are in equilibrium [28].

The *aerodynamic properties* of a canopy needed for the model are the horizontal wind velocity u, the friction velocity u_* and the turbulent diffusivity K. Individual values of these parameters are needed for each height interval Δz. While $u(z)$ is measured at several heights at the site, the K-theory approach is used to calculate $K(z)$ and $u_*(z)$. These expressions include the effect of the thermal stability of the air and are based on the proposals of Goudriaan [29] and Underwood [30]. It is assumed that within canopies the turbulent diffusivity of momentum K_M is equal to K for particles.

It is not possible to compare the results of the model calculation with deposition velocities really measured at forest sites. Published studies of v_d-values above forests do not include descriptions of the canopy in the detail required for the model. Therefore, a one-layer version of the model was tested with the experimental data of Chamberlain [31] describing the particle deposition to artificial grass in a wind tunnel. The agreement was fairly good for particles in large and medium size rages. The modelled deposition of small particles was about 50% lower than the experimental data.

In summarizing, the input parameters which have to be measured in the field are as follows:

- the vertical profile of the horizontal wind velocity u,
- the vertical profile of the temperature T,
- the vertical profile of the vegetation density ρ,
- the orientation and size of the needles,
- the microscale roughness of the needle surface.

2.2. The measuring site

The model was used to calculate the dry deposition of aerosol particles to a spruce stand (*Picea abies* (L.) Karst.) near Wülfersreuth in the subalpine mountainous region Fichtelgebirge, northeastern Bavaria, Germany. The stand, situated at 680 m a.s.l., is an almost rectangular plot 205 m long and 40 m wide. Its longer axis is directed from southwest to northeast. In 1992, when the measurements were made, the age of the trees was about 45 years and their mean height $\bar{h}$ was 20 m. This stand of younger trees was surrounded on all sides by older-grown spruce trees about 25 m high. The ground has an inclination of 5.9° to the northwest [22].

Thus, the site has some horizontal inhomogeneities and is therefore less suitable for micrometeorological investigations. Therefore, the values gained by the model calculation are only valid for the point where the measurements are made, and caution must be exercised in extrapolating them to the whole stand.

2.3. The plant morphology

For determining the vegetation density ρ, the height of the upper and lower boundary of the crown, z_h and z_b, and the cross sectional area A_s of the stem at the height z_b were measured for 29 randomly selected trees. With the regression

$$A_l = 22.6 + 8500 A_s. \tag{6}$$

the leaf area A_l of each individual tree was determined [32]. For distributing this value over the vertical extend of a crown the chi-square-function

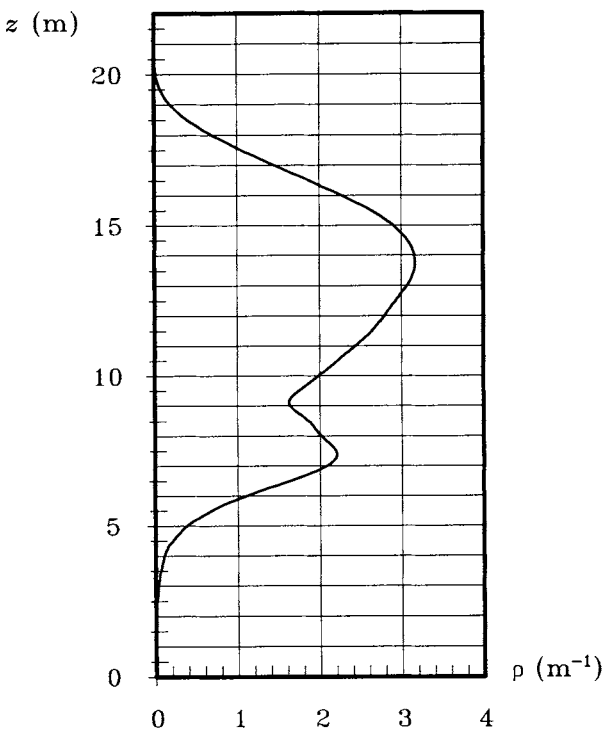

Figure 1. Distribution of the vegetation density ρ with height z at the measuring site

$$\frac{A_l'(z)}{A_l} = \frac{a(z_d)^b \exp(cz_d)}{0.1 \int_{z_b}^{z_h} a(z_d)^b \exp(cz_d) dz} \tag{7}$$

was used [22], where A_l' is the needle surface area per meter tree height, $z_d = (z_h - z)/(z_h - z_b)$, $a = 4.76 \times 10^4$, $b = 6.21$, and $c = -16.23$. After adding the individual distributions for all 29 trees, the overall function $\rho(z)$ shown in Figure 1 was achieved.

By this procedure a surface area index (SAI) of 28.4 was found, and the leaf area index (LAI) was determined to be 11.4 assuming a ratio of total to projected needle area of 2.5.

The average needle diameter d_l was set to 1.5 mm, and it was assumed that the needles do not have any preferred direction in space. The microscale roughness of the needle surface k_s was set to 5 μm which is the elevation of small ridges lying parallel to the needle axis.

2.4. Micrometeorological measurements

Using a tower within the forest stand the horizontal wind velocity was continuously measured by anemometers at heights z of 4.6 m, 11.8 m, 16.6 m, 16.8 m, 18.5 m, 20.2 m, 21.3 m and 28.2 m above the ground. At the uppermost position the wind direction was additionally recorded. At 2.3 m and 20.4 m, i.e. below and above the canopy, the temperature and the relative humidity were measured.

Table 1
Characteristics of the Berner cascade impactors

	5-stage impactor	10-stage impactor
Volumetric flow rate	74.5 l min^{-1}	25.4 l min^{-1}
Cut diameters (μm)	0.05, 0.14, 0.42, 1.2, 3.5, 10.0	0.015, 0.03, 0.06, 0.125, 0.25, 0.5, 1.0, 2.0, 4.0, 8.0, 16.0
Mean diameters (μm)	0.084, 0.24, 0.71, 2.0, 5.9	0.021, 0.042, 0.087, 0.18, 0.35, 0.71, 1.4, 2.8, 5.7, 11.3

2.5. Concentration measurements

Airborne particle-bound concentrations c of the main inorganic ions were measured as a function of the particle diameter d_p by Berner cascade impactors mounted at the top of the canopy. Two different types of impactors were used alternately, one 5-stage impactor ranging from $d_p = 0.05$ μm to 10 μm and one 10-stage impactor ranging from 0.015 μm to 16 μm. Some details about the impactors are listed in Table 1.

The impaction plates were covered by polyethylene film, which after sampling was extracted with deionized water. The solution was analyzed for the ions NH_4^+, K^+, Na^+, SO_4^{2-}, NO_3^-, Cl^- by HPLC with conductivity detectors. For Ca^{2+} and Mg^{2+} ICP-AES analysis was used. By measuring the pH in the solution the concentration of dissociated protons was deduced.

3. RESULTS AND DISCUSSION

From June to November 1992 a total of 23 samples of aerosol particles were taken. The sampling times were on the average 1 day for the 5-stage impactor and 6 days for the 10-stage impactor in accordance with the different flow rate and size partitioning of both devices. These periods covered 23% of a whole year.

3.1. Deposition velocities

For each sampling interval mean values of $v_d(d_p)$ were calculated by the model based on 30-min averages of the meteorological input parameters. To demonstrate the span of the v_d-values that was occurring, the curves for those periods, when the lowest and highest values were found during the measurements, are depicted in Figure 2. The minimum event is an interval lasting 38 hours from June 29 to July 1, 1992. During this period there were fair weather conditions with almost cloudless skies throughout the days and the nights. The wind velocity at $z = 20.2$ m never exceeded 2.0 m s^{-1}. The thermal stratification was very stable. On the other hand, the maximum event, lasting about 6 days from September 29 to October 5, was accompanied by varying thermal stability with long periods of unstable and neutral conditions. The sky was cloudy throughout the interval, and during 3 days the wind velocity was large, reaching values of 5.3 m s^{-1} at $z = 20.2$ m. The difference in v_d between these examples is more than an order of magnitude.

In Figure 2 the curve representing the sum of the mean values and the standard deviation (thin line) is drawn in addition to the mean function of v_d vs d_p (thick line).

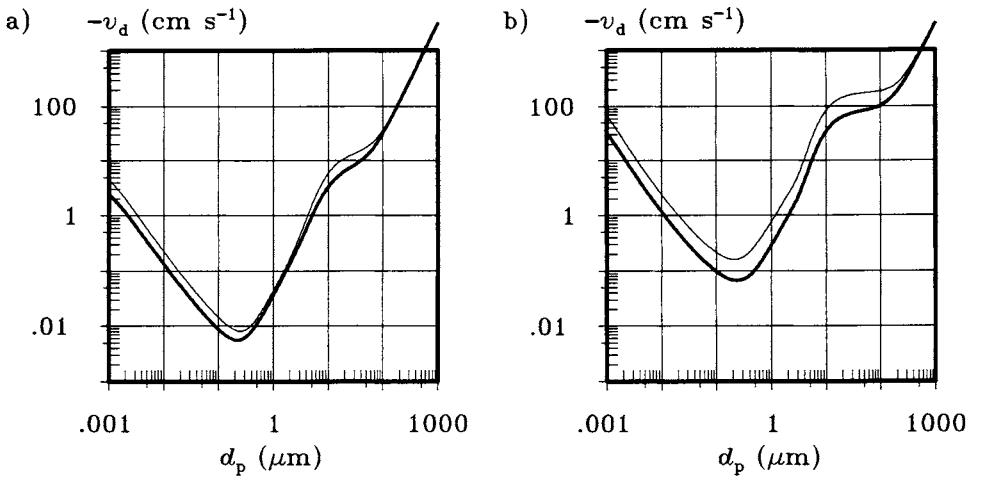

Figure 2. Calculated deposition velocity v_d at the measuring site vs particle diameter d_p. Thick line: mean values; thin line: mean values plus standard deviation. a) measuring period with the smallest v_d; b) measuring period with the largest v_d.

Table 2
Portions in % of equivalent concentrations of particle-bound inorganic ions averaged for all cascade impactor measurements

NH_4^+	Na^+	K^+	Ca^{2+}	Mg^{2+}	H^+	Cations
84	6	2	3	1	4	100
SO_4^{2-}	NO_3^-	Cl^-				Anions
73	22	5				100

This gives an impression of the variability of v_d which is also larger when the mean values are high.

3.2. Particle-bound ion concentrations

The atmospheric content of particle-bound inorganic ions at the measuring site is characterized in Table 2 which lists average portions of equivalent concentrations of the individual substances. It can be concluded that NH_4^+, SO_4^{2-} and NO_3^- are the most important ions. The contributions of sea salt and protons are almost negligible. In general the ion balances of individual samples were in equilibrium, so it does not seem that further important ionic species were overseen.

In Table 3 the mean concentrations of the prevailing ions and some values characterizing their distribution within the particle size spectrum are listed. As a rule of thumb, the geometric mean diameter d_g denotes the particle size where the major portion of the species is occurring. If the size distribution can approximately be described by a log-normal distribution, then d_g is equivalent to the maximum of the distribution. The geometric standard deviation σ_g gives an indication of the spread of the distribution. It can be seen that NO_3^- is on average found in larger particles than SO_4^{2-} and NH_4^+.

Table 3
Average values of airborne concentrations $\bar{c}$, geometric mean diameters $\bar{d}_g$ and geometric standard deviations $\bar{\sigma}_g$, weighted by the measuring time

		5-stage samples	10-stage samples	all samples
NH_4^+	$\bar{c}$ (nmol m^{-3})	152	120	125
	$\bar{d}_g$ (μm)	0.70	0.77	0.76
	$\bar{\sigma}_g$ (μm)	2.14	2.26	2.24
SO_4^{2-}	$\bar{c}$ (nmol m^{-3})	74	51	55
	$\bar{d}_g$ (μm)	0.92	0.90	0.90
	$\bar{\sigma}_g$ (μm)	2.82	2.56	2.60
NO_3^-	$\bar{c}$ (nmol m^{-3})	31	33	33
	$\bar{d}_g$ (μm)	1.59	1.46	1.48
	$\bar{\sigma}_g$ (μm)	2.79	4.13	3.92

The values listed in Table 3 do not show any significant differences between the two cascade impactors. Though the 10-stage impactor covers a broader size range, the mass of sampled material is not larger.

3.3. Deposition fluxes

Deposition fluxes F were calculated according to

$$F = \sum_{i=1}^{n} v_{di} c_i, \tag{8}$$

where n is the number of the impactor stages (5 or 10) and d_{pi} is the particle diameter representing the impactor stage i. A problem arises from the fact that towards lager d_p the deposition velocity increases steeply. Therefore, the particles sampled in the largest stage of the impactors often contribute the largest portion to the deposition flux, even if their fraction of the total particle concentration is low. Hence the choice of d_{pi} for the uppermost impactor stage very sensitively influences the resulting F. In this study the d_{pi} for every stage was set equal to the arithmetic mean of the upper and lower cutoff (see Table 1). It is assumed that the errors resulting from this choice will be compensated if a large number of measurements is averaged.

Another possible procedure is to smooth the impactor data prior to calculation. As is demonstrated in Figure 3, measured size distributions $dc/d\ln d_p$ can sometimes be well fitted by log-normal distributions [33]. Then, upon integration according to

$$F = \int_{0.001\mu m}^{100\mu m} v_g \frac{dc}{dd_p} dd_p \tag{9}$$

the flux F is calculated. However, the majority of the measurements made during this study could not be properly fitted using a log-normal distribution. Therefore, the calculation according to Equation (8) was selected.

In Figure 4 the input fluxes F of NH_4^+-N, NO_3^--N and SO_4^{2-}-S are shown for all sampling periods. The intensities of the fluxes cover a wide range. Maximum values occurred in periods where the ion concentrations in the larger particle size classes was high. As mentioned earlier, the results further reflect the wind velocity and the thermal

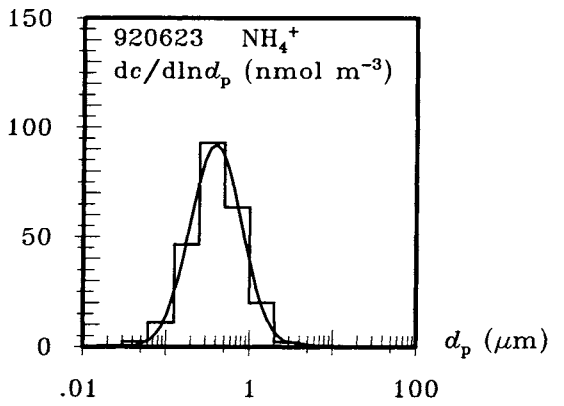

Figure 3. Airborne particle-bound NH_4^+ concentration on June 23 1992 as measured by the 10-stage impactor. The values for the different impactor stages are shown together with the log-normal distribution fitting the measurements.

stability of the air within the canopy. Towards the autumn the fluxes were increased. Note that for the different ions the maxima and minima occurred during different sampling periods. Table 4 lists the mean and maximum fluxes when the results are scaled up to one year.

4. CONCLUSION

The flux values obtained in this study are smaller than those found by a rough estimation made at the same site for the time period from Summer 1988 to Summer 1989 and larger than those found in a similar study conducted in the mountainous region Bavarian Forest [34].

The total (wet and dry) atmospheric input estimated by throughfall analysis at various sites in the Fichtelgebirge amounts to 36 kg ha^{-1} yr^{-1} and 25 kg ha^{-1} yr^{-1} of total sulphur and nitrogen, respectively [35]. This means that the aerosol particle deposition found in this study contributes about 10% to the S deposition and 21% to the N deposition.

It could be suggested that these values are of minor importance as compared to the total input, but one should keep in mind that the role of deposited particles is not defined solely by their contribution to the total ion input to ecosystems. As could be shown by Burkhardt and Eiden [36], the occurrence of thin water films on plant surfaces is enhanced by the presence of deposited particles. In this way the aerosol deposition can also further increase the deposition of gaseous constituents since the gas molecules dissolve in these liquid films.

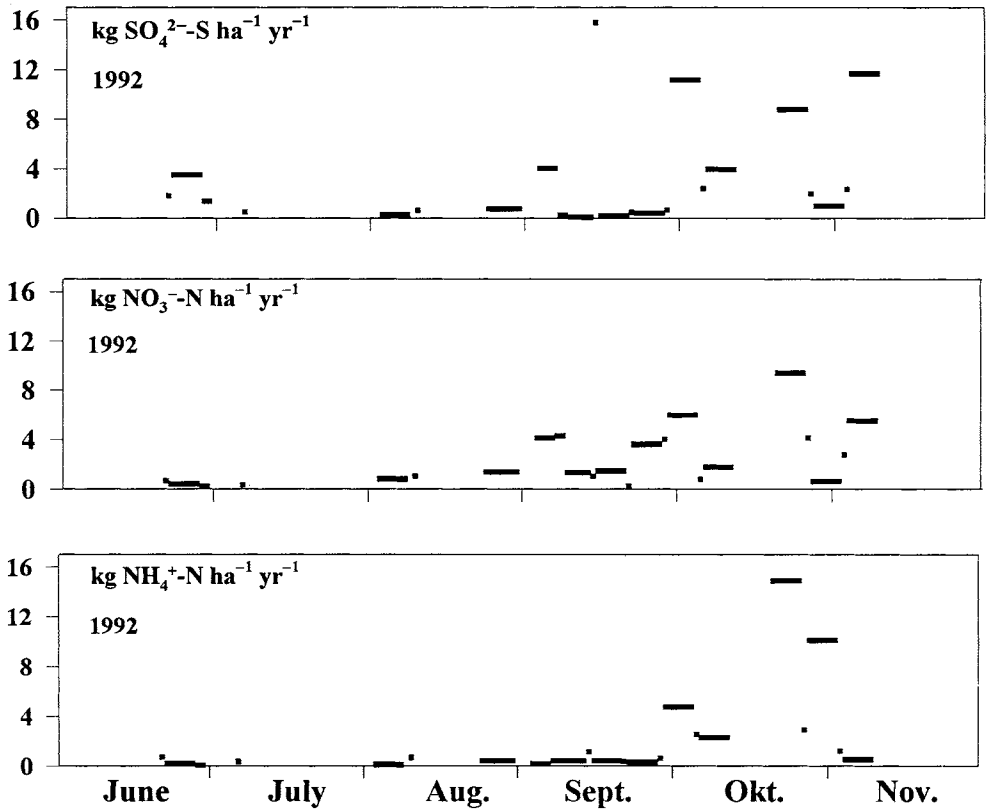

Figure 4. Time courses of the input fluxes of major S and N ions to the spruce forest at Wülfersreuth, Fichtelgebirge

Table 4
Maximum and mean values of yearly input fluxes of the main N and S ions to the spruce stand

	maximum flux F (kg ha^{-1} yr^{-1})	mean flux $\bar{F}$ (kg ha^{-1} yr^{-1})
NH_4^+-N	14.9	2.6
NO_3^--N	9.4	2.7
SO_4^{2-}-S	15.8	3.5

5. ACKNOWLEDGEMENTS

This study was funded by the Bayreuth Institute for Terrestrial Ecosystem Research and thus by the Bundesminister für Forschung und Technologie (grant number PT BEO 51 - 0339476A). Furthermore, thanks are due to Dr. M. McLachlan for final reading of the manuscript.

6. REFERENCES

1 J.W. Erisman, F.A.A.M. de Leeuw and R.M. van Aalst, Atmos. Environ., 23 (1989) 1051.
2 S.E. Lindberg and G.M. Lovett, Atmos. Environ., 26A (1992) 1477.
3 S.E. Lindberg, M. Bredemeier, D.A. Schaefer and L. Qi, Atmos. Environ., 24A (1990) 2207.
4 K.W. Nicholson, Atmos. Environ., 22 (1988) 2653.
5 B.B. Hicks, D.R. Matt, R.T. McMillen, J.D. Womack, M.L. Wesely, R.L. Hart, D.R. Cook, S.E. Lindberg, R.G. de Pena and D.W. Thomson, J. Geophys. Res., 94D (1989) 13003.
6 A. Bytnerowicz, P.J. Dawson, C.L. Morrison and M.P. Poe, Atmos. Environ., 25A (1991) 2203.
7 G.M. Lovett and S.E. Lindberg, Atmos. Environ., 26A (1992) 1469.
8 B. Ulrich, in *Effects of Accumulation of Air Pollutants in Forest Ecosystems*, B. Ulrich and J. Pankrath Eds., Reidel, Dordrecht, 1983, pp. 33 – 45.
9 R. Mayer, Staub Reinh. Luft, 45 (1985) 267.
10 G.M. Lovett and S.E. Lindberg, J. Appl. Ecol., 21 (1984) 1013.
11 B. Duan, C.W. Fairall and D.W. Thomson, J. Appl. Meteorol., 27 (1988) 642.
12 I.Y. Lee and M.L. Wesely, J. Appl. Meteorol., 28 (1989) 176.
13 R. Lorenz and C.E. Murphy Jr., Boundary-Layer Meteorol., 46 (1989) 355.
14 A.G. Allen, R.M. Harrison and K.W. Nicholson, Atmos. Environ., 25A (1991) 2671.
15 B.B. Hicks, D.D. Baldocchi, T.P. Meyers, R.P. Hosker Jr. and D.R. Matt, Wat. Air Soil Poll., 36 (1987) 311.
16 J.W. Erisman, A. van Pul and P. Wyers, in *Air Pollution Research Report 47*, J. Slanina, G. Angeletti and S. Beilke Eds., E. Guyot, Brussels, 1993, pp. 215 – 234.
17 D.H. Bache, Atmos. Environ., 13 (1979) 1257.
18 D.H. Bache, Atmos. Environ., 13 (1979) 1681.
19 D.H. Bache, Atmos. Environ., 18 (1984) 2517.
20 W.G.N. Slinn, Atmos. Environ., 16 (1982) 1785.
21 B.L.B. Wiman and G.I. Ågren, Atmos. Environ., 19 (1985) 335.
22 K. Peters and R. Eiden, Atmos. Environ., 26A, (1992) 2555.
23 S.K. Friedlander and H.F. Johnstone, Ind. Eng. Chem., 49 (1957) 1151.
24 N.B. Wood, J. Aerosol Sci., 12 (1981) 275.
25 S.J. Kline, W.C. Reynolds, F.A. Schraub and P.W. Runstadler, J. Fluid Mech., 30 (1967) 741.
26 K.R. May and R. Clifford, Ann. occup. Hyg., 10 (1967) 83.
27 Y. Belot and D. Gauthier, in *Heat and Mass Transfer in the Biosphere* Part 1, D.A. de Vries and N.H. Afgan Eds., Wiley, New York, 1975, pp. 583 – 591.
28 H.R. Pruppacher and J.D. Klett, Microphysics of Clouds and Precipitation, Reidel, Dordrecht, 1978.

29 J. Goudriaan, Crop Micrometeorology: a Simulation Study, Pudoc, Wageningen, 1977.
30 B.Y. Underwood, Atmos. Environ., 21 (1987) 1573.
31 A.C. Chamberlain, Proc. Roy. Soc. A, 296 (1967) 45.
32 G. Bauer, University of Bayreuth, Chair of Plant Ecology I, personnel communication.
33 L. Gomes, G. Bergametti, F. Dulac and U. Ezat, J. Aerosol Sci., 21 (1990) 47.
34 K. Peters, J. Ludwig and K. Ruoß, J. Aerosol Sci., 22 (1991) S569.
35 B. Manderscheid and E. Matzner, Spatial and Temporal Variability of Soil Solution Chemistry and Seepage Water Ion Fluxes in a Mature Norway Spruce (Picea abies (L.) Karst.) Stand, submitted to Biogeochemistry 1994.
36 J. Burkhardt and R. Eiden, Atmos. Environ., 28 (1994) 2001.